

Supporting Information for

A new steady-state gas/particle partitioning model of PAHs: Implication for the influence of the particulate proportion in emissions

Fu-Jie Zhu^{a,b}, Peng-Tuan Hu^{a,c}, Wan-Li Ma^{a,b,*}

^a International Joint Research Center for Persistent Toxic Substances (IJRC-PTS), State Key Laboratory of Urban Water Resource and Environment, Harbin Institute of Technology, Harbin 150090, China

^b Heilongjiang Provincial Key Laboratory of Polar Environment and Ecosystem (HPKL-PEE), Harbin 150090, China

^c School of Environment, Key Laboratory for Yellow River and Huai River Water Environment and Pollution Control, Ministry of Education, Henan Normal University, Xinxiang, China

*Corresponding author. International Joint Research Center for Persistent Toxic Substances (IJRC-PTS), State Key Laboratory of Urban Water Resource and Environment, Harbin Institute of Technology, 73 Huanghe Road, Nangang District, Harbin 150090, Heilongjiang, China.

Email address: mawanli002@163.com

14	S1. Texts	
15	Text S1. The introduction of the steady-state six-compartment six-fugacity model.....	3
16	Text S2. The calculation method of the output and input fluxes for the particle phase and the	
17	gas phase compartments	7
18	Text S3. The expression of the $\log K_P$ using fugacity method	8
19	Text S4. The introduction of the prediction models	9
20	Text S5. The calculation method of the root mean square error.....	10
21	S2. Tables	
22	Table S1 The transport parameter D (mol/(Pa·h)) for the multimedia fugacity model.....	11
23	Table S2. The fugacity capacity Z values and the partition parameter K values for the	
24	multimedia fugacity model	13
25	Table S3. The partition parameter K values for the multimedia fugacity model.....	14
26	Table S4. The values of A and B for the PAHs.....	15
27	Table S5. The half-lives of 15 PAHs in different phases (h^{-1}).....	16
28	Table S6. The environmental parameters for the multimedia fugacity model	17
29	S3. Figures	
30	Fig. S1. Comparison of the fluxes for the input and output fluxes of the gas phase and	
31	particle phase	19
32	Fig. S2. The difference between the new steady-state model with the H-B model and the L-	
33	M-Y model	20
34	Fig. S3. The comparison between the monitored data of $\log K_P$ of PAHs from 11 cities in	
35	China and the prediction lines of the new steady-state model with different values of ϕ_0	21
36	Fig. S4. The values of $RMSE$ for the new steady-state model based on the monitored data	
37	from 11 cities in China	22
38	Fig. S5. The comparison between the monitored data of $\log K_P$ of PAHs from a coking plant	
39	and the prediction lines of the new steady-state model with different values of ϕ_0 (left panel)	
40	and the related values of $RMSE$ of the new steady-state model (right panel)	23
41	Fig. S6. The comparison between the monitored data of $\log K_P$ of PBDEs from E-waste	
42	sites and the prediction lines of the new steady-state model with different values of ϕ_0 ..	24
43	Fig. S7. The values of the $RMSE$ of the new steady-state model based on the monitored	
44	data of PBDEs from e-waste sites	25
45	References	26
46		

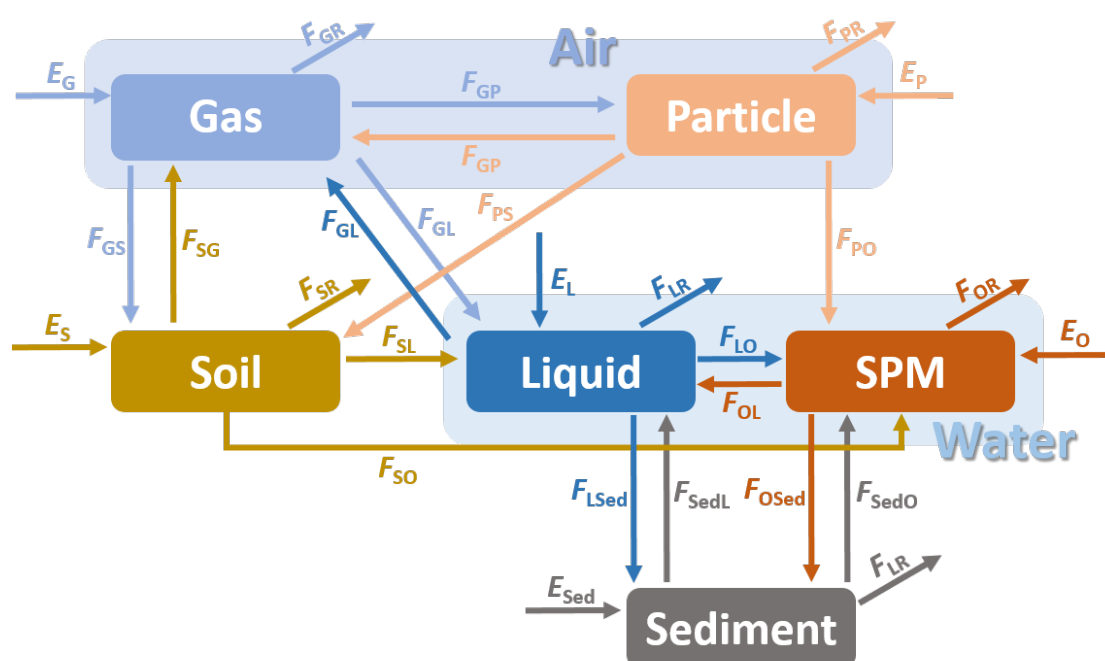
S1. Texts

Text S1. The introduction of the steady-state six-compartment six-fugacity model

Multimedia fugacity models have been used to address chemical pollution by providing a quantitative account of the sources, transport processes, fate and sinks of organic chemicals (Mackay, 2001). A steady-state six-compartment (gas, particle, liquid, suspended particle matter (SPMs), soil, sediments) six-fugacity model was derived using the fugacity theory (Li et al., 2021b). The six-compartment six-fugacity system was exhibited in following figure. The subscripts represent different environment matrix: gas (G), liquid (L), soil (S), sediment (Sed), particle in air (P), and particle in liquid (O). The primary equation in fugacity models is the relationship between the flux (F) and the fugacity (f):

$$F = fD \quad (S1)$$

where D is the intermedia D values defined in the fugacity theory (Mackay, 2001).



The six-compartment six-fugacity system

(Notes: E_i is the emission rate (mol/h) to compartment i ; F_{ij} is the flux from compartment i to compartment j (mol/h); F_{iR} is the flux by reaction (mol/h); Particle represents particle in air; SPM represents suspended particle matter in water.)

The relationships between the above figure (focusing on the processes related to the six compartments) in Supporting Information and Fig.1 (focusing on the processes related to gas and particle phases) in the main text of the manuscript were described in detail as follows. For the gas phase, in the above figure, the flux of F_{GS} (flux from gas to soil) includes the diffusion flux from gas to soil (F_{GS_diff}) and the wet deposition flux from gas to soil (F_{GS_w}). The flux of F_{GL} (flux from gas to liquid) includes the diffusion flux from gas to soil (F_{GW_diff}) and the wet deposition flux from gas to liquid (F_{GW_w}). In the Fig. 1, the corresponding flux F_{GSW_diff} is the sum of F_{GS_diff} and F_{GW_diff} . F_{GW} is the sum of F_{GS_w} and F_{GW_w} . For the particle phase, in the above figure, the flux of F_{PO} (flux from particle to SPMs) includes wet deposition flux from particle to SPMs (F_{PO_w}) and dry deposition flux from particle to SPMs (F_{PO_D}). The flux of F_{PS} (flux from particle to soil) includes wet deposition flux from particle to soil (F_{PS_w}) and dry deposition flux from particle to soil (F_{PS_D}). In the Fig. 1, the corresponding flux F_{PD} is the sum of F_{PO_D} and F_{PS_D} . The flux F_{PW} is the sum of F_{PO_w} and F_{PS_w} .

Once the relationships between the six compartments were confirmed, the function between the total input flux and the total output flux can be established for each compartment. The relationship follows the general form:

$$E_i + \sum D_{ji}f_j = \sum D_{ik}f_i + D_{iR}f_i \quad (S2)$$

where, E_i is the emission rate (mol/h) to compartment i; D_{ji} is the intermedia D values from compartment j to compartment i (mol/(Pa·h)); D_{ik} is the intermedia D values from compartment i to compartment k (mol/(Pa·h)); D_{iR} is the reaction rate D value in compartment i (mol/(Pa·h)); f_i and f_j are the fugacity of chemical in compartment i and compartment j (Pa).

In the present study, both the gaseous and particulate emissions were considered in the models. Therefore, the above equation for each compartment can be expressed as follows in detail:

Air: Gas phase:

$$E_G + D_{LG}f_L + D_{SG}f_S + D_{PG}f_P = (D_{GL} + D_{GS} + D_{GP} + D_{GR})f_G \quad (S3)$$

Air: Particle phase:

$$E_P + D_{GP}f_G = (D_{PG} + D_{PS} + D_{PO} + D_{PR})f_P \quad (S4)$$

Water: Dissolved phase:

$$D_{GL}f_G + D_{SL}f_S + D_{SedL}f_{Sed} + D_{OL}f_O = (D_{LG} + D_{LSed} + D_{LO} + D_{LR})f_L \quad (S5)$$

Water: Solid phase:

$$D_{LO}f_L + D_{SO}f_S + D_{SedO}f_{Sed} + D_{PO}f_P = (D_{OL} + D_{OSed} + D_{OR})f_O \quad (S6)$$

Soil phase:

$$D_{GS}f_G + D_{PS}f_P = (D_{SG} + D_{SL} + D_{SO} + D_{SR})f_S \quad (S7)$$

Sediment phase:

$$D_{LSed}f_S + D_{OSed}f_O = (D_{SedL} + D_{SedO} + D_{SedR})f_{Sed} \quad (S8)$$

where D values for each intermedia process were given in **Table S1**.

The fugacity capacity Z values of each compartment used for calculation of the D values can be obtained by the equations in **Table S2**. The parameters for PAHs and environment were given in **Tables S3, S4 S5 and S6**. In the present study, the unit of the system was assumed as a cuboid with the air surface area (A_A) of 1 m², water surface area (A_W) of 0.7 m², and soil surface area (A_S) of 0.3 m². The height and/or depth of air, water and soil are 1000, 10 and 0.15 m, respectively.

The fugacity for each compartment can be obtained by analyzing the above equations. Then the parameters of each compartment and the parameters between

112 different compartments can be calculated, such as fluxes, concentrations, mass fractions,
113 and partitioning behavior (Qin et al., 2021; Li et al., 2021b; Li et al., 2021a).

114

Text S2. The calculation method of the output and input fluxes for the particle phase and the gas phase compartments

The 11 output and input fluxes for the particle phase and the gas phase can be calculated by the following equations:

$$(1 - \phi_0)E = E_G \quad (S9)$$

$$\phi_0 E = E_P \quad (S10)$$

$$F_{GP} = D_{GP} f_G \quad (S11)$$

$$F_{PG} = D_{GP} f_P \quad (S12)$$

$$F_{Gdiff} = (D_{GDL} + D_{GDS}) f_G \quad (S13)$$

$$F_{GW} = (D_{GWL} + D_{GWS}) f_G \quad (S14)$$

$$F_{diffG} = D_{LG} f_L + D_{SG} f_S \quad (S15)$$

$$F_{PD} = (D_{PDO} + D_{PDS}) f_P = D_{PD} f_P \quad (S16)$$

$$F_{PW} = (D_{PWO} + D_{PWS}) f_P = D_{PW} f_P \quad (S17)$$

$$F_{GR} = D_{GR} f_G \quad (S18)$$

$$F_{PR} = D_{PR} f_P \quad (S19)$$

where the D values can be found in **Table S1**.

Text S3. The expression of the log K_P using fugacity method

The G/P partitioning coefficient (K_P) can be calculated as follows:

$$K_P = (C_P/C_G)/TSP \quad (S20)$$

where C_P (ng/m³ air) and C_G (ng/m³) are the PAHs concentrations in particle phase and gas phase, respectively, and TSP is the concentrations of total suspended particles (μg/m³).

C_P can be transferred to C'_P (ng/m³ particle) based the following equation:

$$C_P = C'_P \times TSP/10^9 \rho_P \quad (S21)$$

where C'_P (ng/m³ particle) is the PAHs concentrations in particle phase with different units, and ρ_P is the density of particles (kg/m³).

Then, the Eq. (S20) can be expressed in different form:

$$K_P = (C'_P/C_G)/10^9 \rho_P \quad (S22)$$

The ratio of C'_P to C_G can be calculated using the method from the multimedia fugacity model:

$$C'_P/C_G = f_P Z_P / f_G Z_G \quad (S23)$$

where Z_P/Z_G equal to K_{PG} at equilibrium state, which can be calculated by the following equation (Li et al., 2015):

$$K_{PG} = Z_P/Z_G = 10^9 \rho_P K_{P-HB} \quad (S24)$$

where K_{P-HB} is the G/P partitioning coefficient calculated from the H-B model (the equilibrium-state model) (Harner and Bidleman, 1998b).

Summarizing the equations above, log K_P can be expressed as following equation:

$$\log K_P = \log K_{P-HB} + \log(f_P/f_G) \quad (S25)$$

Text S4. The introduction of the prediction models

The H-B model

Under assumptions that the dominate G/P distribution process was absorption and the system was in *equilibrium-state*, an equation (named as the *H-B* model in the present study) used to predict the value of K_P for SVOCs was derived in an early study (Harner and Bidleman 1998b)

$$\log K_{P-HB} = \log K_{OA} + \log f_{OM} - 11.91 \quad (S26)$$

The L-M-Y model

Li et al. established a *steady-state* model (named as the *L-M-Y* model in the present study) for the investigation of the G/P partitioning behavior of PBDEs (Li et al. 2015). The influences of dry and wet depositions of particles on the G/P partitioning were considered in the *L-M-Y* model. A non-equilibrium parameter caused by dry and wet depositions of particles, $\log \alpha$ was introduced into the *L-M-Y* model:

$$\log K_{P-LMY} = \log K_{P-HB} + \log \alpha \quad (S27)$$

$$\log \alpha = -\log(1 + 4.18 \times 10^{-11} f_{OM} K_{OA}) \quad (S28)$$

Therefore, the *H-B* model is a special case of the *L-M-Y* model when the non-equilibrium term ($\log \alpha$) equal zero.

Text S5. The calculation method of the root mean square error

To evaluate the performance of the new steady-state model, the root mean square error (*RMSE*) was calculated based on the following equation:

$$RMSE = \sqrt{\frac{1}{n} \sum (\log K_{P-P} - \log K_P)^2} \quad (S29)$$

where $\log K_{P-P}$ is the prediction data from the new steady-state model, and $\log K_P$ is the monitored data.

The smaller of the *RMSE* value indicated the better matching degree between the predicted data and the monitored data.

S2. Tables

Table S1 The transport parameter D (mol/(Pa·h)) for the multimedia fugacity model

Compartments	Symbol	D values	Process
Gas-Liquid	D_{GDL}	$1/[1/(k_{\text{VG}}A_{12}Z_{\text{G}})+1/(k_{\text{VW}}A_{12}Z_{\text{W}})]$	Diffusion
	D_{GWL}	$A_{12}U_{\text{R}}Z_{\text{W}}$	Rain dissolution
	D_{GL}	$D_{\text{GDL}}+D_{\text{GWL}}$	Gas \rightarrow Liquid
	D_{LG}	D_{GDL}	Liquid \rightarrow Gas
	D_{GDS}	$1/[1/(k_{\text{EG}}A_{13}Z_{\text{G}})+Y_3/[A_{13}(B_{\text{MG}}Z_{\text{G}}+B_{\text{MW}}Z_{\text{W}})]]$	Diffusion
Gas-Soil	D_{GWS}	$A_{13}U_{\text{R}}Z_{\text{W}}$	Rain dissolution
	D_{GS}	$D_{\text{GDS}}+D_{\text{GWS}}$	Gas \rightarrow Soil
	D_{SG}	D_{GDS}	Soil \rightarrow Gas
	D_{PWO}	$A_{12}U_{\text{R}}Q_{\text{VP}}Z_{\text{P}}$	Wet deposition
Particles-SPMs	D_{PDO}	$A_{12}U_{\text{D}}v_{\text{P}}Z_{\text{P}}$	Dry deposition
	D_{PO}	$D_{\text{PWO}}+D_{\text{PDO}}$	Particle \rightarrow SPMs
	D_{PWS}	$A_{13}U_{\text{R}}Q_{\text{VP}}Z_{\text{P}}$	Wet deposition
Particles-Soil	D_{PDS}	$A_{13}U_{\text{D}}v_{\text{P}}Z_{\text{P}}$	Dry deposition
	D_{PS}	$D_{\text{PWS}}+D_{\text{PDS}}$	Particle \rightarrow Soil
	D_{PG}	$A_{\text{P}}k_{\text{PG}}Z_{\text{G}}$	Sorption and desorption
Gas-Particles	D_{GP}	D_{PG}	Gas \rightarrow Particle
	D_{PG}	D_{PG}	Particle \rightarrow Gas
Soil-Liquid	D_{SL}	$A_{13}U_{\text{WW}}Z_{\text{W}}$	Water runoff
	D_{SL}	D_{SL}	Soil \rightarrow Liquid
Soil-SPMs	D_{SO}	$A_{13}U_{\text{EW}}Z_{\text{S}}$	Soil runoff
	D_{SO}	D_{SO}	Soil \rightarrow SPM
Liquid-SPMs	D_{LO}	$A_{\text{O}}k_{\text{WO}}Z_{\text{W}}$	Sorption and desorption

continued Table S1

Compartments	Symbol	D values	Process
	D_{LO}	D_{LO}	Liquid \rightarrow SPMs
	D_{OL}	D_{LO}	SPMs \rightarrow Liquid
Sediment-Liquid	D_{SedL}	$1/[1/(k_{SW}A_{24}Z_W)+Y_4/(B_M wA_{24}Z_W)]$	diffusion
	D_{SedL}	D_{SedL}	Liquid \rightarrow Sediment
	D_{LSed}	D_{SedL}	Sediment \rightarrow Liquid
	D_{OSed}	$U_{DO}A_{24}Z_O$	Deposition
Sediment-SPMs	D_{SedO}	$U_{RS}A_{24}Z_{Sed}$	Resuspension
	D_{OSed}	D_{OSed}	SPMs \rightarrow Sediment
	D_{SedO}	D_{SedO}	Sediment \rightarrow SPMs
Degradation	D_{iR}	$k_{degi}V_iZ_i$	Degradation in compartment i

185 Notes: The gaseous degradation rate of PAHs can be calculated using the half-lives of PAHs: k_{degi}
186 $= \ln(2)/t_{1/2}$ (The half-lives of the 15 PAHs can be found in **Table S5**).

187 **Table S2. The fugacity capacity Z values and the partition parameter K values for**
188 **the multimedia fugacity model**

Z	Equation	Unit
Z_G	$1/RT$	mol/(m ³ ·Pa)
Z_W	$1/H$ or Z_G/K_{AW}	mol/(m ³ ·Pa)
Z_S	$K_{SG}Z_G$	mol/(m ³ ·Pa)
Z_{sed}	$K_{SedW}Z_W$	mol/(m ³ ·Pa)
Z_P	$K_{PG}Z_G$	mol/(m ³ ·Pa)
Z_O	$K_{PW}Z_W$	mol/(m ³ ·Pa)

189

190 **Table S3. The partition parameter K values for the multimedia fugacity model**

K Process	K	Equation	Unit
Soil-Gas	K_{SG}	$f_{OM(S)}K_{OA}$	dimensionless
Sediment-Liquid	K_{SedW}	$f_{OC(Sed)}K_{OC}\rho_{Sed}/1000$	dimensionless
Gas-Particle	K_{PG}	$10^{-2.91}\rho_P f_{OM}K_{OA}$	dimensionless
SPMs-Liquid	K_{PW}	$f_{OC(O)}\rho_O K_{OC}/1000$	dimensionless
Organic carbon-Water	K_{OC}	$0.41(L/kg)K_{OW}$	L/kg
Air-Water	K_{AW}	$\log K_{AW} = A_{AW} + B_{AW} / T_W$	dimensionless
Octanol-Water	K_{OW}	$\log K_{OW} = A_{OW} + B_{OW} / T_W$	dimensionless
Octanol-Air	K_{OA}	$\log K_{OA} = A_{OA} + B_{OA} / T$	dimensionless

191 Note: T and T_W are the temperature in atmosphere and in water, respectively, K; The values of T
192 equal to T_W when the temperature in air higher than 0°C, and the value of T_W equal to the constant
193 value when the temperature in air lower than 0°C.; The values of A and B for the calculation of K_{AW} ,
194 K_{OW} , K_{OA} can be calculated (See details in **Table S4**).

195 **Table S4. The values of A and B for the PAHs**

PAHs	Abbreviations	A_{AW}	B_{AW}	A_{OW}	B_{OW}	A_{OA}	B_{OA}
acenaphthylene	Acy	5.46	-2272	1.67	593	-1.97	2476
acenaphthene	Ace	5.66	-2251	1.43	774	-2.20	2597
fluorene	Flu	5.97	-2483	1.56	816	-2.61	2833
phenanthrene	Phe	6.06	-2607	1.49	944	-3.37	3293
anthracene	Ant	6.14	-2620	1.73	867	-3.41	3316
fluoranthene	Fluo	6.44	-2850	0.83	1295	-4.34	3904
pyrene	Pyr	6.29	-2780	1.09	1182	-4.56	3985
benzo[a]anthracene	BaA	7.10	-3222	0.99	1453	-5.64	4746
chrysene	Chr	7.01	-3205	0.91	1499	-5.65	4754
benzo[b]fluoranthene	BbF	7.39	-3438	-0.33	1847	-6.40	5285
benzo[k]fluoranthene	BkF	7.47	-3458	0.10	1870	-6.42	5301
benzo[a]pyrene	BaP	7.25	-3374	0.32	1709	-6.50	5382
indeo[1,2,3-cd]pyrene	IcdP	7.63	-3614	-0.73	2177	-7.00	5791
dibenzo[a,h]anthracene	DahA	7.97	-3805	0.52	1986	-7.17	5887
benzo[g,h,j]perylene	BghiP	7.41	-3526	-0.67	2245	-7.03	5834

196 Note: The values of A_{OA} and B_{OA} were cited from references (Odabasi et al., 2006; Harner and
197 Bidleman, 1998a), except the values for Nap were calculated by the equations: $B_X =$
198 $U_X/(\ln(10)*8.314)$, $A_X = \log K_X(25^\circ\text{C}) - B_X/298.15$ (X represent AW, OW, and OA). A_{OW} and B_{OW}
199 were also calculated using the above equations. The values in the equations ($\log K_X$, U_X) were
200 calculated using the UFZ - LSER Database
201 ([https://www.ufz.de/index.php?en=31698&contentonly=1&m=0&lserd_data\[mvc\]=Public/start](https://www.ufz.de/index.php?en=31698&contentonly=1&m=0&lserd_data[mvc]=Public/start)).
202 A_{AW} and B_{AW} were calculated by the equations: $A_{AW} = A_H - 3.351$, $B_{AW} = B_H$ (A_H and B_H were
203 parameters used for the calculation of the Henry's Law constants (Parnis et al., 2016), $\log K_{AW} =$
204 $\log H - \log (R^*T)$, $\log (R^*T) \approx 3.351$ when temperature ranged from 223 K to 323 K). \log
205 $K_{OW}(25^\circ\text{C})$ for BbF and IcdP were cited from the reference (Ma et al., 2010). U_{OW} for BbF and IcdP
206 were calculated from $U_{OW} = U_{OA} + U_{AW}$.

207 **Table S5. The half-lives of 15 PAHs in different phases (h⁻¹)**

PAHs	t_A	t_W	t_S	t_{Sed}	t_P	t_O
Acy	1.70	360	7.20×10^2	3.24×10^3	7.20×10^2	3.24×10^3
Ace	1.92	900	1.80×10^3	8.10×10^3	1.80×10^3	8.10×10^3
Flu	14.5	360	7.20×10^2	3.24×10^3	7.20×10^2	3.24×10^3
Phe	9.87	1440	2.88×10^3	1.30×10^4	2.88×10^3	1.30×10^4
Ant	3.21	1440	2.88×10^3	1.30×10^4	2.88×10^3	1.30×10^4
Fluo	4.39	1440	2.88×10^3	1.30×10^4	2.88×10^3	1.30×10^4
Pyr	2.57	1440	2.88×10^3	1.30×10^4	2.88×10^3	1.30×10^4
BaA	2.57	1440	2.88×10^3	1.30×10^4	2.88×10^3	1.30×10^4
Chr	2.57	1440	2.88×10^3	1.30×10^4	2.88×10^3	1.30×10^4
BbF	6.92	1440	2.88×10^3	1.30×10^4	2.88×10^3	1.30×10^4
BkF	2.39	1440	2.88×10^3	1.30×10^4	2.88×10^3	1.30×10^4
BaP	2.57	1440	2.88×10^3	1.30×10^4	2.88×10^3	1.30×10^4
IcdP	1.99	1440	2.88×10^3	1.30×10^4	2.88×10^3	1.30×10^4
DahA	2.57	1440	2.88×10^3	1.30×10^4	2.88×10^3	1.30×10^4
BghiP	1.48	1440	2.88×10^3	1.30×10^4	2.88×10^3	1.30×10^4

208 Note: The data were cited from the Estimation Programs Interface (EPI) Suite TM (the US
209 Environmental Protection Agency's Office of Pollution Prevention and Toxics and Syracuse
210 Research Corporation (SRC)).

211

212 **Table S6. The environmental parameters for the multimedia fugacity model**

Parameters	Description	Value	Unit	Function
k_{VG}	Gas side MTC over water	3	m/h	
k_{VW}	Liquid side MTC	0.03	m/h	
U_R	Rainfall rate	9.70×10^{-5}	m/h	
Q	Scavenging ratio	2×10^5	–	
v_P	Volume fraction of aerosol particle	6.67×10^{-11}	–	$10^{-9} TSP / \rho_P$
U_D	Dry deposition velocity	10.8	m/h	
k_{EG}	Gas side MTC over soil	1	m/h	
Y_3	Diffusion path length in soil	0.05	m	
B_{MG}	Molecular diffusivity in gas	0.04	m ² /h	
B_{MW}	Molecular diffusivity in liquid	4.00×10^{-6}	m ² /h	
U_{WW}	Liquid runoff rate from soil	3.90×10^{-5}	m/h	
U_{EW}	Solids runoff rate from soil	2.30×10^{-8}	m/h	
k_{SW}	Liquid side MTC over sediment	0.01	m/h	
Y_4	Diffusion path length in sediment	0.005	m	
U_{DO}	SPMs deposition rate	4.60×10^{-8}	m/h	
U_{RS}	Sediment resuspension rate	1.10×10^{-8}	m/h	
k_{PG}	Gas-Particle Partitioning MTC	1.89×10^1	m/h	$C B_{PG} / l_{PG}$
B_{PG}	Molecular diffusivity in air	1.80×10^{-2}	m ² /h	
l_{PG}	Air boundary layer thickness	4.75×10^{-3}	m	
C	Accommodation coefficient	5	–	
k_{WO}	Solid-Dissolved Partitioning MTC	4.21×10^{-3}	m/h	$C' B_{WO} / l_{WO}$
B_{WO}	Molecular diffusivity in water	4.00×10^{-6}	m ² /h	
l_{WO}	Water boundary layer thickness	4.75×10^{-3}	m	
C'	Accommodation coefficient	5	–	
$\rho_P / \rho_O / \rho_{Sed}$	Density of particles in air and water and sediment	1.50×10^3	kg/m ³	
d_P / d_O	Diameter of particles in air and water	1.00×10^{-7}	m	
TSP	Concentration of particles in air	1.00×10^2	ug/m ³	
SPM	Concentration of particles in water	10	g/m ³	

continued Table S6

Parameters	Description	Value	Unit	Function
$f_{OC(O)}$	Fraction of organic carbon in SPMs	0.04	–	
$f_{OM(S)}$	Fraction of organic materials in soil	0.04	–	
$f_{OC(Sed)}$	Fraction of organic carbon in sediment	0.1	–	
A_P	Total area of particles in air	4	m ²	$6 \times 10^{-9} TSP \times V_G / (\rho_P d_P)$
A_O	Total area of particles in Water	2800	m ²	$6 \times 10^{-3} SPM \times V_w / (\rho_O d_O)$

213 Note: The values of the parameters were cited from Mackay (2001) (Mackay, 2001).

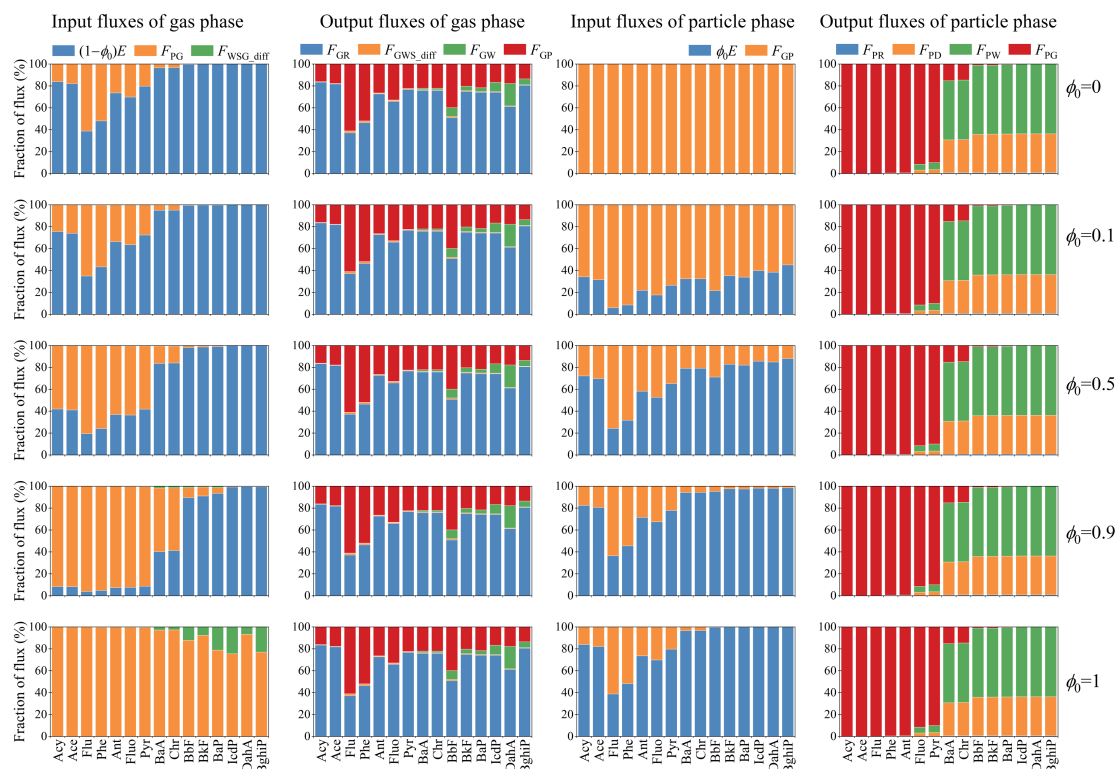


Fig. S1. Comparison of the fluxes for the input and output fluxes of the gas phase and particle phase

Note: F_{GR} : degradation flux of gas phase PAHs; F_{PR} : degradation flux of particle phase PAHs; F_{GP} : migration flux from gas phase to particle phase; F_{PG} : migration flux from particle phase to gas phase; F_{GWS_diff} : diffusion fluxes from gas phase to water and soil phases; F_{GW} : wet deposition flux of gas phase PAHs; F_{WSG_diff} : diffusion fluxes from soil and water phases to gas phase; F_{PD} : dry deposition flux of particle phase PAHs; F_{PW} : wet deposition flux of particle phase PAHs; $(1-\phi_0)E$: emission flux of gas phase PAHs; ϕ_0E : emission flux of particle phase PAHs.

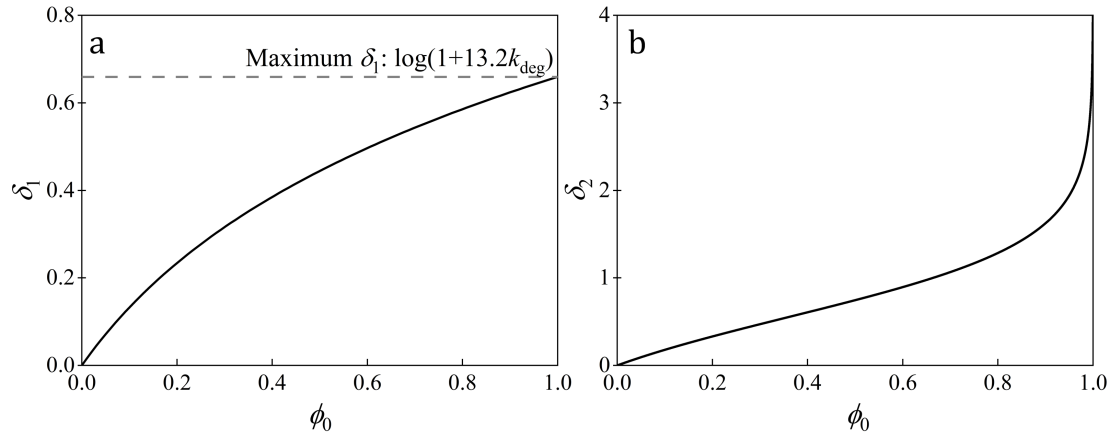


Fig. S2. The difference between the new steady-state model with the H-B model and the L-M-Y model

Note: δ_1 and δ_2 were calculated based on the value of $k_{deg} = 0.27 \text{ h}^{-1}$, δ_1 is the difference between the new steady-state model with the H-B model and the L-M-Y model when $\log K_{OA} < \log K_{OA1}$, and δ_2 is the difference between the new steady-state model with the L-M-Y model when $\log K_{OA} > \log K_{OA2}$.

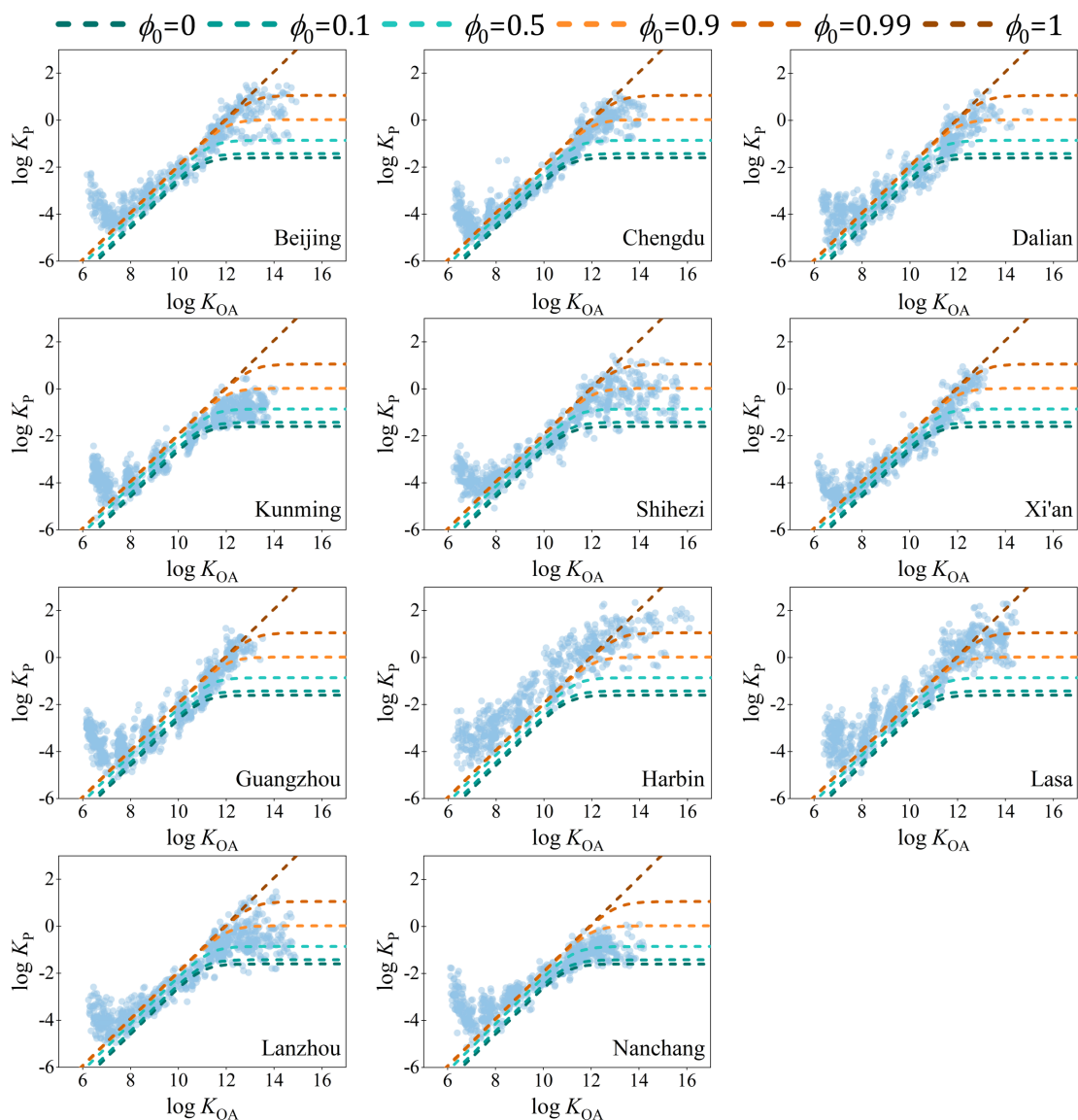


Fig. S3. The comparison between the monitored data of $\log K_P$ of PAHs from 11 cities in China and the prediction lines of the new steady-state model with different values of ϕ_0 .

Note: the k_{deg} of 0.27 h^{-1} and f_{OM} of 0.21 were used in the new steady-state model.

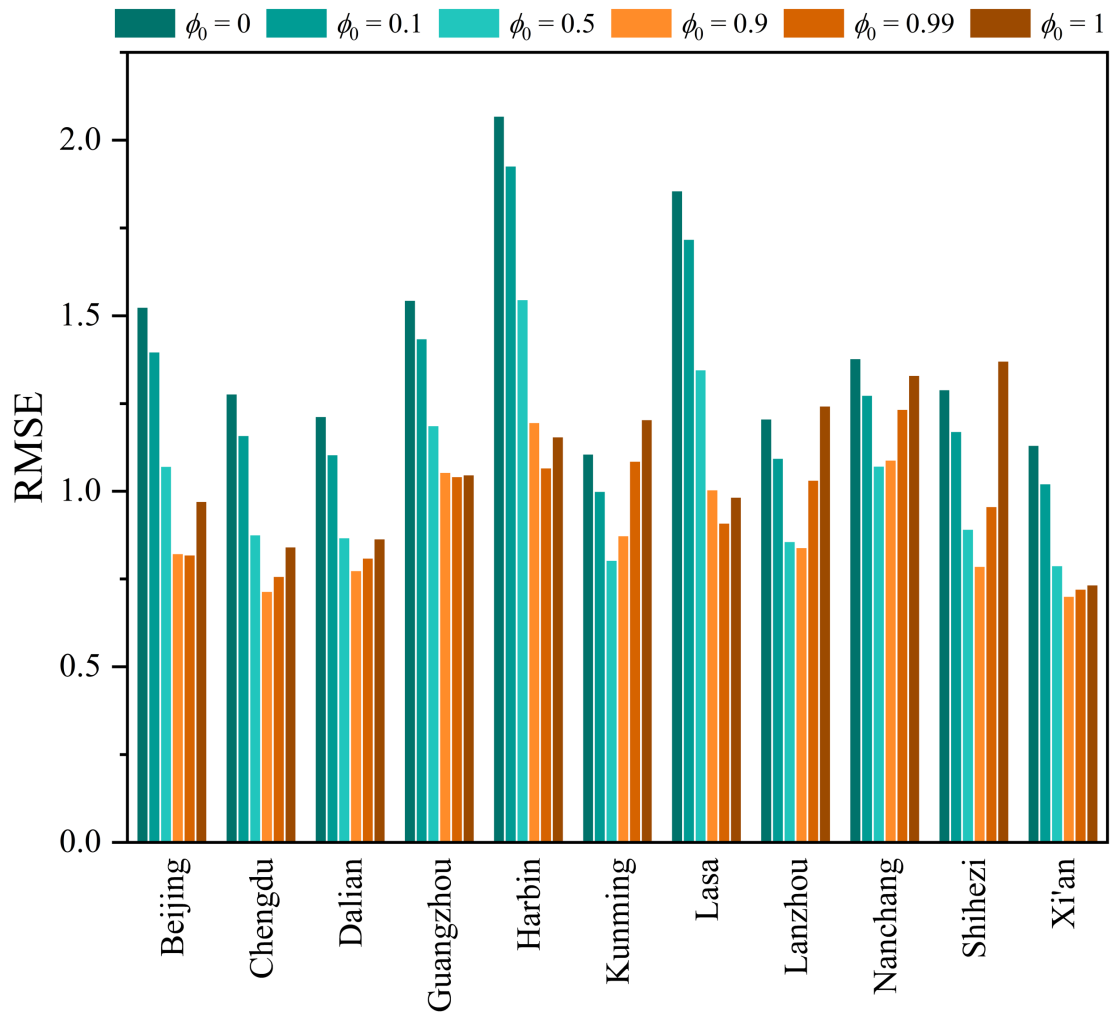


Fig. S4. The values of $RMSE$ for the new steady-state model based on the monitored data from 11 cities in China

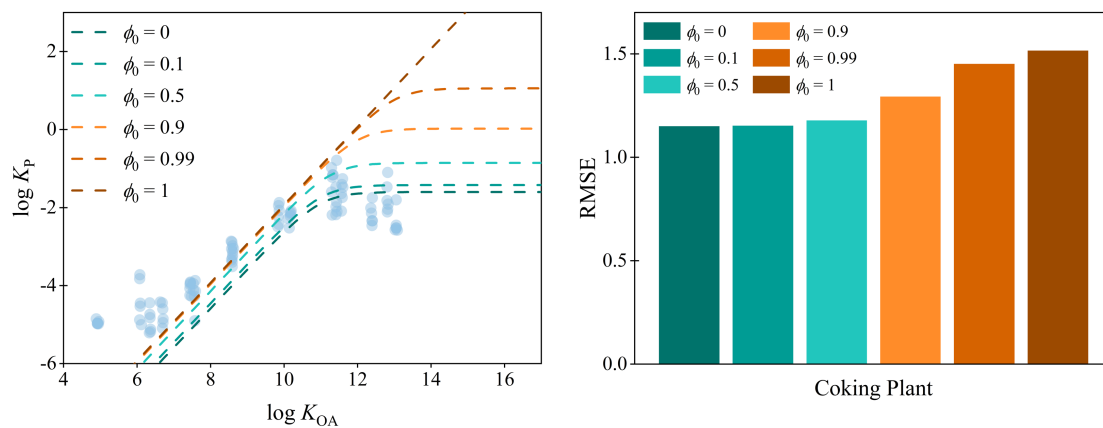


Fig. S5. The comparison between the monitored data of $\log K_P$ of PAHs from a coking plant and the prediction lines of the new steady-state model with different values of ϕ_0 (left panel) and the related values of $RMSE$ of the new steady-state model (right panel)

Note: The k_{deg} of 0.27 h^{-1} and f_{OM} of 0.21 were used in the new steady-state model; and the monitored data were cited from a coking plant(Liu et al., 2019).

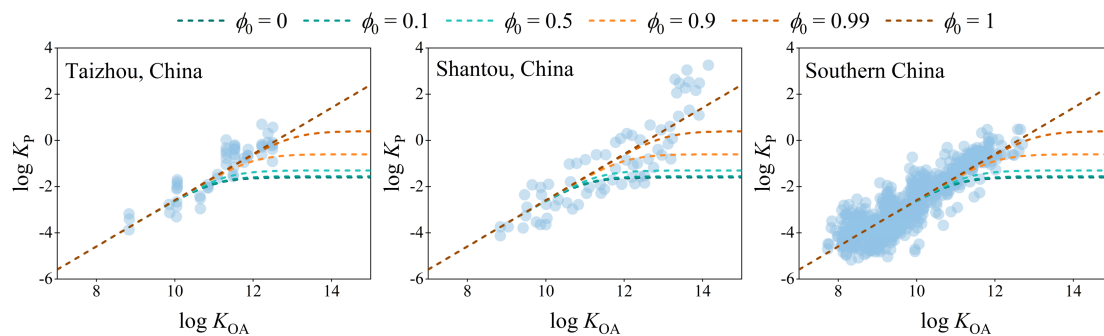


Fig. S6. The comparison between the monitored data of $\log K_P$ of PBDEs from E-waste sites and the prediction lines of the new steady-state model with different values of ϕ_0

Note: The k_{deg} of 0.27 h^{-1} and f_{OM} of 0.21 were used in the new steady-state model; and the monitored data were cited from the following references: Taizhou, China(Han et al., 2009); Shantou, China(Chen et al., 2011); and Southern China(Tian et al., 2011).

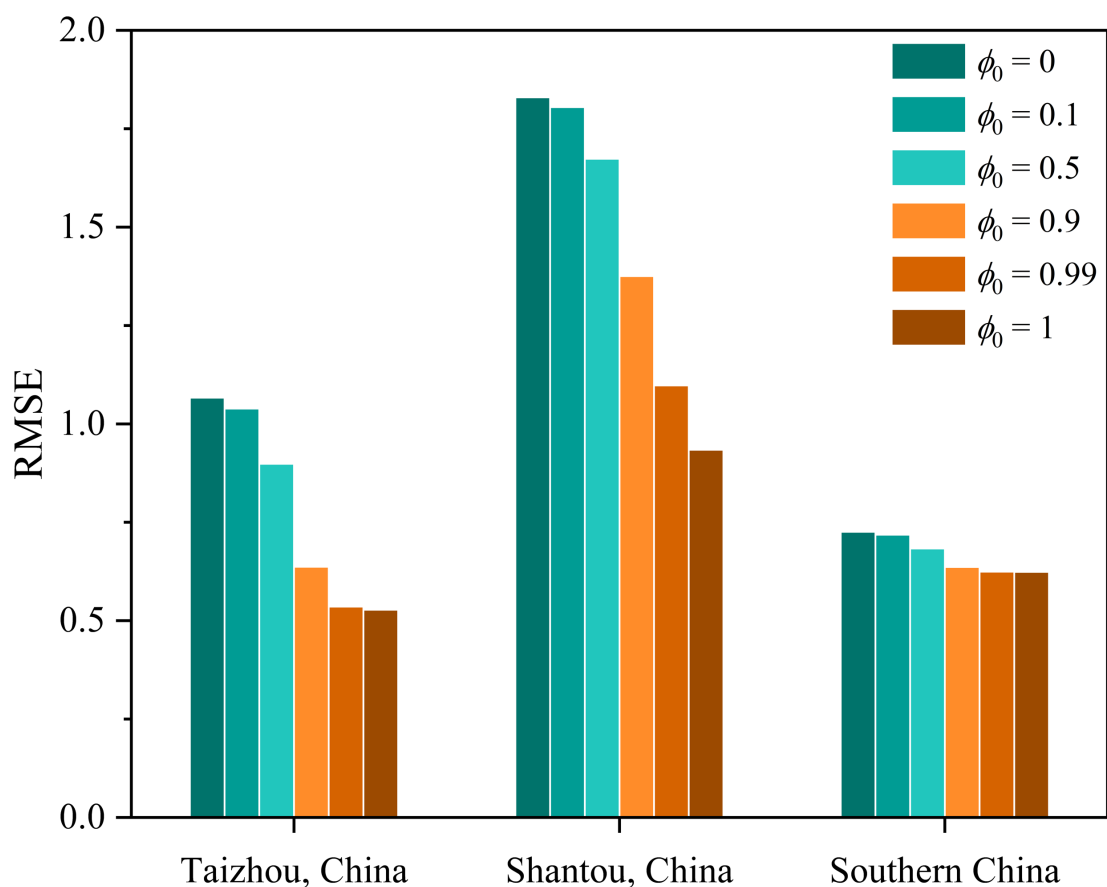


Fig. S7. The values of the *RMSE* of the new steady-state model based on the monitored data of PBDEs from e-waste sites

257 References

- 258 Chen, D., Bi, X., Liu, M., Huang, B., Sheng, G., and Fu, J.: Phase partitioning, concentration
259 variation and risk assessment of polybrominated diphenyl ethers (PBDEs) in the
260 atmosphere of an e-waste recycling site, *Chemosphere*, 82, 1246-1252,
261 <https://doi.org/10.1016/j.chemosphere.2010.12.035>, 2011.
- 262 Han, W., Feng, J., Gu, Z., Chen, D., Wu, M., and Fu, J.: Polybrominated Diphenyl Ethers in the
263 Atmosphere of Taizhou, a Major E-Waste Dismantling Area in China, *Bul . Environ.*
264 *Contam. Toxicol.*, 83, 783-788, 10.1007/s00128-009-9855-9, 2009.
- 265 Harner, T. and Bidleman, T. F.: Measurement of Octanol-Air Partition Coefficients for
266 Polycyclic Aromatic Hydrocarbons and Polychlorinated Naphthalenes, *Journal of*
267 *Chemical & Engineering Data*, 43, 40-46, 10.1021/jc970175x, 1998a.
- 268 Harner, T. and Bidleman, T. F.: Octanol-air partition coefficient for describing particle/gas
269 partitioning of aromatic compounds in urban air, *Environ. Sci. Technol.*, 32, 1494-1502,
270 1998b.
- 271 Li, Y.-F., Qin, M., Yang, P.-F., Hao, S., and Macdonald, R. W.: Particle/gas partitioning for semi-
272 volatile organic compounds (SVOCs) in Level III multimedia fugacity models: Gaseous
273 emissions, *Sci. Total Environ.*, 795, 148729,
274 <https://doi.org/10.1016/j.scitotenv.2021.148729>, 2021a.
- 275 Li, Y.-F., Qin, M., Yang, P.-F., Liu, L.-Y., Zhou, L.-J., Liu, J.-N., Shi, L.-L., Qiao, L.-N., Hu, P.-T., Tian,
276 C.-G., Nikolaev, A., and Macdonald, R.: Treatment of particle/gas partitioning using level
277 III fugacity models in a six-compartment system, *Chemosphere*, 271, 129580,
278 <https://doi.org/10.1016/j.chemosphere.2021.129580>, 2021b.
- 279 Li, Y. F., Ma, W. L., and Yang, M.: Prediction of gas/particle partitioning of polybrominated
280 diphenyl ethers (PBDEs) in global air: A theoretical study, *Atmospheric Chemistry and*
281 *Physics*, 15, 1669-1681, 10.5194/acp-15-1669-2015, 2015.
- 282 Liu, X., Zhao, D., Peng, L., Bai, H., Zhang, D., and Mu, L.: Gas-particle partition and spatial
283 characteristics of polycyclic aromatic hydrocarbons in ambient air of a prototype coking
284 plant, *Atmos. Environ.*, 204, 32-42, <https://doi.org/10.1016/j.atmosenv.2019.02.012>,
285 2019.
- 286 Ma, Y.-G., Lei, Y. D., Xiao, H., Wania, F., and Wang, W.-H.: Critical Review and Recommended
287 Values for the Physical-Chemical Property Data of 15 Polycyclic Aromatic Hydrocarbons
288 at 25 degrees C, *J. Chem. Eng. Data*, 55, 819-825, 10.1021/jc900477x, 2010.
- 289 Mackay, D.: *Multimedia Environmental Models: the Fugacity Approach*, Taylor & Francis, New
290 York 2001.
- 291 Odabasi, M., Cetin, E., and Sofuoglu, A.: Determination of octanol-air partition coefficients and
292 supercooled liquid vapor pressures of PAHs as a function of temperature: Application to
293 gas-particle partitioning in an urban atmosphere, *Atmos. Environ.*, 40, 6615-6625,
294 10.1016/j.atmosenv.2006.05.051, 2006.
- 295 Parnis, J. M., Mackay, D., and Harner, T.: Temperature dependence of Henry's law constants
296 and K-OA for simple and heteroatom-substituted PAHs by COSMO-RS (vol 110, pg 27,
297 2015), *Atmos. Environ.*, 136, 21-21, 10.1016/j.atmosenv.2016.04.009, 2016.
- 298 Qin, M., Yang, P. F., Hu, P. T., Hao, S., Macdonald, R. W., and Li, Y. F.: Particle/gas partitioning
299 for semi-volatile organic compounds (SVOCs) in level III multimedia fugacity models: Both
300 gaseous and particulate emissions, *Sci. Total Environ.*, 790, 148012,
301 <https://doi.org/10.1016/j.scitotenv.2021.148012>, 2021.
- 302 Tian, M., Chen, S.-J., Wang, J., Zheng, X.-B., Luo, X.-J., and Mai, B.-X.: Brominated Flame
303 Retardants in the Atmosphere of E-Waste and Rural Sites in Southern China: Seasonal
304 Variation, Temperature Dependence, and Gas-Particle Partitioning, *Environ. Sci. Technol.*,
305 45, 8819-8825, 10.1021/es202284p, 2011.
- 306